Journal of Sound and Vibration (1998) **211**(4), 593–605

ENERGY FLOW ANALYSIS OF COUPLED BEAMS

P. E. Cho

Case Corporation, Technology Center, 7 S. 600 County Line Road, Hinsdale, IL 60521, *U.S.A.*

AND

R. J. Bernhard

Ray W. Herrick Laboratories, School of Mechanical Engineering, Purdue University, West Lafayette, IN 47907-1077, *U.S.A.*

(*Received* 13 *December* 1996, *and in final form* 8 *October* 1997)

Energy flow analysis (EFA) is an analytical tool for prediction of the frequency-averaged vibrational response of built-up structures at high audible frequencies. The procedure is based on two developments; first, the derivation of the partial differential equations that govern the propagation of energy-related quantities in simple structural elements such as rods, beams, plates, and acoustic cavities; and second, the derivation of coupling relationships in terms of energy-related quantities that describe the transfer of energy for various joints (e.g., beam-to-beam, rod-to-beam, plate-to-plate, structure-to-acoustic field coupling). In this investigation, the energy flow coupling relationships at these joints for rods and beams are derived. EFA is used to predict the frequency-averaged vibrational response of a frame structure with a three-dimensional joint, where four wave types propagate in the structure. The predicted results of EFA are shown to be a good approximation of the frequency-averaged "exact" energetics, which are computed from classical displacement solutions.

1. INTRODUCTION

There are currently no simple methods for predicting the vibrational and acoustical response of built-up structures such as automobiles, aircrafts, and ships throughout the entire audible frequency range. The finite element method (FEM) and the boundary element method (BEM) are effective for the prediction of vibrational and acoustical response of built-up structures at low frequencies. However, at high frequencies, FEM/BEM are ineffective due to the requirement that the mesh size is small, which makes model generation, turn-around time, and computational cost relatively high. Moreover, studies [1, 2] have shown that the measured frequency response functions (FRF) of air-borne and structure-borne transmission paths of nominally identical automotive vehicles vary 5–10 dB above 200 Hz. Consequently, a deterministic prediction of vibrational and acoustical response of built-up structures at high frequencies using FEM or BEM will not be particularly useful.

At high frequencies, it would be useful for design purposes to know the space- and frequency-average vibrational behavior of a structure. One approach to predict such responses is energy flow analysis (EFA) [3–8]. The basic premise of EFA is that the state of vibration can be essentially represented by stored, dissipated, and transferred farfield energy densities. EFA is used to predict the space- and frequency-averaged vibrational behavior of a structure in much the same manner as statistical energy analysis (SEA)

0022–460X/98/140593 + 13 $25.00/0/sv971350

[9–11]. However, the governing differential equations of EFA are derived using a differential volume approach. Thus, the spatial variation of farfield energy density and energy flow is predicted. The advantages of using a differential equation to describe the state of farfield vibrational energy is that effects such as localized damping and power inputs can be modelled in a straightforward fashion. The power transmission and reflection coefficients (for structure to structure coupling) and radiation efficiencies (for structure to acoustic space coupling) are used to couple simple structural and/or acoustical elements together [12–16]. Hence, the power transmission and reflection coefficients and radiation efficiencies of various types of coupled structures published in the literature can be readily incorporated for use in EFA.

In this investigation, the vibrational response of a frame structure with a three-dimensional joint is predicted using EFA. Due to the geometry of the joint, vibrational energy conversions occur at the joint of the frame structure which causes propagation of four types of vibrational energy transmission mechanisms within the structure. EFA is used to predict all four types of energy transmission propagating in the frame structure and to identify the dominant vibrational energy transmission mechanisms in the frame structure.

2. THEORY

2.1. GOVERNING DIFFERENTIAL EQUATIONS

To develop the governing energy differential equation for one-dimensional structural elements (i.e., rods and beams), first, an energy balance over a one-dimensional differential element is performed. The time rate of change of energy per unit length in the one-dimensional differential element must equal the difference in energy entering and leaving the differential element minus the power dissipated due to damping within the differential element. Hence, the resulting energy balance can be represented as [5, 6]

$$\frac{\partial e}{\partial t} = -\frac{\partial q}{\partial x} - \pi_{diss}, \tag{1}$$

where e is the energy per unit length, q is the power, and π_{diss} is the power dissipated due to damping. For steady state conditions, the time rate of change of energy density is zero.

For a loss factor damping model, the time averaged power dissipated in the differential element is proportional to the local energy per unit length [13],

$$\langle \pi \rangle_{diss} = \eta \omega \langle e \rangle, \tag{2}$$

where η is the structural loss factor and ω is the circular frequency.

If the vibrational energy of a finite structure is segregated into positive and negative traveling components, the power (or energy flow) and energy per unit length are related by [13]

$$\langle q \rangle^+ = c_g \langle e \rangle^+ \qquad \text{and} \qquad \langle q \rangle^- = -c_g \langle e \rangle^-, \tag{3, 4}$$

where c_g is the group velocity of the type of wave propagating in the structure, and $\langle e \rangle^+$ and $\langle e \rangle^-$ are positive and negative components of traveling energy per unit length. The expressions of group velocities for flexural, longitudinal, and torsional waves are, respectively,

$$c_{gfm} = 2\left[\frac{\omega^2 E I_i}{\rho S}\right]^{1/4}, \qquad c_{gl} = \sqrt{\frac{ES}{\rho S}}, \qquad \text{and} \qquad c_{gt} = \sqrt{\frac{G}{\rho}}, \tag{5–7}$$

where the subscript, m, is the direction of transverse displacement ($m = x$, y or z), the subscript, i, is the axis of area moment of inertia normal to the direction of the transverse displacement ($i = x$, y or z), ρ is the material density, S is the cross-sectional area, I_i is the area moment of inertia, E is Young's modulus, and G is the shear modulus.

When equations (2)–(4) are substituted into equation (1), two first order energy differential equations can be obtained,

$$\frac{\mathrm{d}}{\mathrm{d}x}(c_g\langle e\rangle^+) + \eta\omega\langle e\rangle^+ = 0 \qquad \text{and} \qquad -\frac{\mathrm{d}}{\mathrm{d}x}(c_g\langle e\rangle^-) + \eta\omega\langle e\rangle^- = 0, \qquad (8, 9)$$

The general solution of equations (8) and (9) are

$$\langle e\rangle^+ = A\exp\left(-\frac{\eta\omega}{c_g}x\right) \qquad \text{and} \qquad \langle e\rangle^- = B\exp\left(\frac{\eta\omega}{c_g}x\right), \qquad (10, 11)$$

where the constants, A and B, are determined by energy per unit length or energy flow boundary conditions. For finite structures, both positive and negative propagating waves exist. Since the frequency-averaged vibrational response of finite structures approach those of similar infinite structures, the general solutions (10) and (11) can be used to predict the frequency-averaged energy per unit length and energy flow distributions in a finite structure. The approximate energy per unit length distribution is the scalar sum of $\langle e\rangle^+$ and $\langle e\rangle^-$. The approximate net energy flow (or power) distribution is the vector sum of $\langle q\rangle^+$ and $\langle q\rangle^-$.

2.2. ENERGY FLOW COUPLING RELATIONSHIPS AT A JOINT

Waves propagating in structures eventually encounter changes in material, geometry, or structural configuration (i.e., a bend, a T-joint, or an L-joint). These discontinuities are referred to as joints in this study. The coupling relationships are used to describe the energy density and energy flow on either side of the joint.

The wave transmission approach is used extensively in the vibro-acoustic field to estimate the power transmission and reflection coefficients (also, known as efficiencies) of a joint [12–16]. In a finite structure, as in the coupled rods case shown in Figure 1, the waves (which carry energy) incident upon the joint will produce partially reflected waves in rod 1 and transmitted waves in rod 2. The transmitted waves will encounter the boundary in rod 2 and will be reflected. The reflected waves in rod 2 will be re-incident upon the joint, which will produce partially transmitted waves past the joint toward rod 1 and reflected waves in rod 2. The primary reflected waves in rod 1 will encounter the boundary of rod 1 and will be reflected. The secondary reflected waves in rod 1 will be re-incident upon the joint. This process will continue as long as the excitation source continually injects power into the structure.

This process can be adequately described by the semi-infinite rod joint model shown in Figure 2, where an incident wave from each rod simultaneously impinges upon the joint

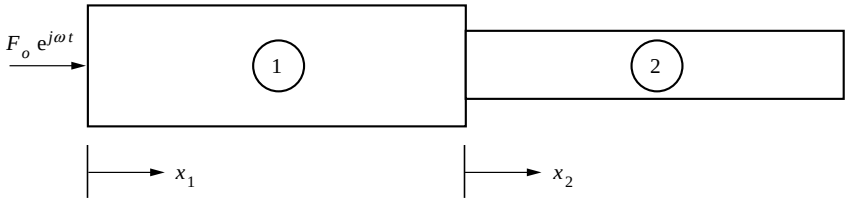

Figure 1. Two coupled collinear rods.

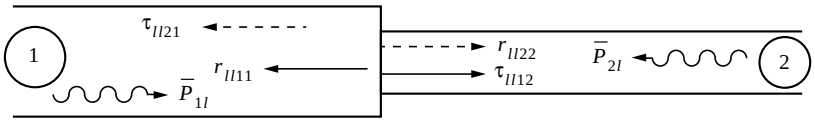

Figure 2. Longitudinal power transmission and reflection coefficients resulting from an incident longitudinal wave in each rod; $\bar{P}_{1l}$ = incident longitudinal wave in rod 1, $\bar{P}_{2l}$ = incident longitudinal wave in rod 2, r_{ll11} = reflected longitudinal wave in rod 1, r_{ll22} = reflected longitudinal wave in rod 2, τ_{ll21} = transmitted longitudinal wave from rod 2 to rod 1, τ_{ll12} = transmitted longitudinal wave from rod 1 to rod 2.

from each direction. The left traveling wave incident upon the joint will be partially reflected and partially transmitted. The right traveling wave incident upon the joint will also be partially reflected and partially transmitted. Hence, the left traveling energy flow in rod 1 can be represented as the sum of contributions from the partially reflected right traveling wave in rod 1 and the partially transmitted left traveling wave of rod 2. The right traveling energy flow in rod 2 can be represented as the sum of contributions from the partially reflected left traveling wave in rod 2 and the partially transmitted traveling wave of rod 1. The fraction of the incident wave which is transmitted and reflected past a joint can be determined from wave transmission analysis. Hence, the net energy flow away from the joint in each rod can be represented as

$$\langle q\rangle_2^- = \tau_{ll12}\langle q\rangle_1^+ + r_{ll22}\langle q\rangle_2^+, \qquad \langle q\rangle_1^- = r_{ll11}\langle q\rangle_1^+ + \tau_{ll21}\langle q\rangle_2^+ \tag{12, 13}$$

where t_{llij} is the power transmission coefficient of longitudinal waves from rod i to rod j $(i, j = 1, 2)$ and r_{llii} is the power reflection coefficient for longitudinal waves in rod i. The positive energy flow is considered as the energy flow incident upon the joint. The negative energy flow is considered as the energy flow moving away from the joint. For one-dimensional structures, $t_{ij} = t_{ji}$ and $r_{ii} = r_{jj}$. Hence, only one set of power transmission and reflection coefficients needs to be computed. Since for conservative joints, the sum of t_{12} and r_{12} is one, the addition of equations (12) and (13) yield the energy flow balance relationship at the joint,

$$\langle q\rangle_1^+ - \langle q\rangle_1^- - \langle q\rangle_2^+ + \langle q\rangle_2^- = 0. \tag{14}$$

Equation (14) is a reiteration of conservation of energy flow across the joint. At the joint, the difference of energy flow of positive and negative propagating waves in rod 1 is equal to the difference in energy flow in rod 2. Hence, equations (12) and (13) are an alternative representation of the principle of conservation of energy.

By using power transmission and reflection coefficients to model the energy flow across the joint, a large amount of published literature on wave transmission analysis of various types of coupled structures can be incorporated into EFA. Also, as power transmission and reflection coefficients are used for structure-to-structure coupling, it is believed that radiation efficiencies can be used for structure-to-acoustic space coupling.

For coupled structures of higher complexities, such as beams joined at arbitrary angles and branched beam systems, the energy flow coupling relationships at the joint become more complex. When two beams are joined at an arbitrary angle, both longitudinal and flexural waves propagate in the structure due to the geometry of the joint. The net energy flow in the receiving beam is a sum of contributions from the incident, transmitted, and reflected flexural and longitudinal waves. In branched beam systems, the net energy flow away from the joint must account for the contributions, not only from the propagation of both the longitudinal and flexural waves in the structure, but also from the extra branched beams in the structure. For the beam joint shown in Figure 3, two flexural waves, one longitudinal wave, and one torsional wave propagate in the frame structure due to

the geometry of the joint. Hence, the energy flow on either side of the joint must account for the contributions from all four types of waves. The net flexural, longitudinal, and torsional energy flow away from the joint in each beam section can be represented as

$$\langle q\rangle^{-}_{3fz} = \tau_{fzfz23}\langle q\rangle^{+}_{2fz} + \tau_{fyfz23}\langle q\rangle^{+}_{2fy} + \tau_{lfz23}\langle q\rangle^{+}_{2l} + \tau_{tfz23}\langle q\rangle^{+}_{2t} + \tau_{fxfz43}\langle q\rangle^{+}_{4fx} + \tau_{fyfz43}\langle q\rangle^{+}_{4fy}$$
$$+ \tau_{lfz43}\langle q\rangle^{+}_{4l} + \tau_{tfz43}\langle q\rangle^{+}_{4t} + r_{fzfz33}\langle q\rangle^{+}_{3fz} + r_{fxfz33}\langle q\rangle^{+}_{3fx} + r_{lfz33}\langle q\rangle^{+}_{3l} + r_{tfz33}\langle q\rangle^{+}_{3t},$$

$$\langle q\rangle^{-}_{3fx} = \tau_{fzfx23}\langle q\rangle^{+}_{2fz} + \tau_{fyfx23}\langle q\rangle^{+}_{2fy} + \tau_{lfx23}\langle q\rangle^{+}_{2l} + \tau_{tfx23}\langle q\rangle^{+}_{2t} + \tau_{fxfx43}\langle q\rangle^{+}_{4fx}$$
$$+ \tau_{fyfx43}\langle q\rangle^{+}_{4fy} + \tau_{lfx43}\langle q\rangle^{+}_{4l} + \tau_{tfx43}\langle q\rangle^{+}_{4t} + r_{fzfx33}\langle q\rangle^{+}_{3fz}$$
$$+ r_{fxfx33}\langle q\rangle^{+}_{3fx} + r_{lfx33}\langle q\rangle^{+}_{3l} + r_{tfx33}\langle q\rangle^{+}_{3t},$$

$$\langle q\rangle^{-}_{3l} = \tau_{fzl23}\langle q\rangle^{+}_{2fz} + \tau_{fyl23}\langle q\rangle^{+}_{2fy} + \tau_{ll23}\langle q\rangle^{+}_{2l} + \tau_{tl23}\langle q\rangle^{+}_{2t} + \tau_{fxl43}\langle q\rangle^{+}_{4fx} + \tau_{fyl43}\langle q\rangle^{+}_{4fy}$$
$$+ \tau_{ll43}\langle q\rangle^{+}_{4l} + \tau_{tl43}\langle q\rangle^{+}_{4t} + r_{fzl33}\langle q\rangle^{+}_{3fz} + r_{fxl33}\langle q\rangle^{+}_{3fx} + r_{ll33}\langle q\rangle^{+}_{3l} + r_{tl33}\langle q\rangle^{+}_{3t},$$

$$\langle q\rangle^{-}_{3t} = \tau_{fzt23}\langle q\rangle^{+}_{2fz} + \tau_{fyt23}\langle q\rangle^{+}_{2fy} + \tau_{lt23}\langle q\rangle^{+}_{2l} + \tau_{tt23}\langle q\rangle^{+}_{2t} + \tau_{fxt43}\langle q\rangle^{+}_{4fx} + \tau_{fyt43}\langle q\rangle^{+}_{4fy}$$
$$+ \tau_{lt43}\langle q\rangle^{+}_{4l} + \tau_{tt43}\langle q\rangle^{+}_{4t} + r_{fzt33}\langle q\rangle^{+}_{3fz} + r_{fxt33}\langle q\rangle^{+}_{3fx} + r_{lt33}\langle q\rangle^{+}_{3l} + r_{tt33}\langle q\rangle^{+}_{3t},$$

$$\langle q\rangle^{-}_{2fz} = r_{fzfz22}\langle q\rangle^{+}_{2fz} + r_{fyfz22}\langle q\rangle^{+}_{2fy} + r_{lfz22}\langle q\rangle^{+}_{2l} + r_{tfz22}\langle q\rangle^{+}_{2t} + \tau_{fxfz42}\langle q\rangle^{+}_{4fx} + \tau_{fyfz42}\langle q\rangle^{+}_{4fy}$$
$$+ \tau_{lfz42}\langle q\rangle^{+}_{4l} + \tau_{tfz42}\langle q\rangle^{+}_{4t} + \tau_{fzfz32}\langle q\rangle^{+}_{3fz} + \tau_{fxfz32}\langle q\rangle^{+}_{3fx} + \tau_{lfz32}\langle q\rangle^{+}_{3l} + \tau_{tfz32}\langle q\rangle^{+}_{3t},$$

$$\langle q\rangle^{-}_{2fy} = r_{fzfy22}\langle q\rangle^{+}_{2fz} + r_{fyfy22}\langle q\rangle^{+}_{2fy} + r_{lfy22}\langle q\rangle^{+}_{2l} + r_{tfy22}\langle q\rangle^{+}_{2t} + \tau_{fxfy42}\langle q\rangle^{+}_{4fx}$$
$$+ \tau_{fyfy42}\langle q\rangle^{+}_{4fy} + {}_{lfy42}\langle q\rangle^{+}_{4l} + \tau_{tfy42}\langle q\rangle^{+}_{4t} + \tau_{fzfy32}\langle q\rangle^{+}_{3fz}$$
$$+ \tau_{fxfy32}\langle q\rangle^{+}_{3fx} + \tau_{lfy32}\langle q\rangle^{+}_{3l} + \tau_{tfy32}\langle q\rangle^{+}_{3t},$$

$$\langle q\rangle^{-}_{2l} = r_{fzl22}\langle q\rangle^{+}_{2fz} + r_{fyl22}\langle q\rangle^{+}_{2fy} + r_{ll22}\langle q\rangle^{+}_{2l} + r_{tl22}\langle q\rangle^{+}_{2t} + \tau_{fxl42}\langle q\rangle^{+}_{4fx} + \tau_{fyl42}\langle q\rangle^{+}_{4fy}$$
$$+ \tau_{ll42}\langle q\rangle^{+}_{4l} + \tau_{tl42}\langle q\rangle^{+}_{4t} + \tau_{fzl32}\langle q\rangle^{+}_{3fz} + \tau_{fxl32}\langle q\rangle^{+}_{3fx} + \tau_{ll32}\langle q\rangle^{+}_{3l} + \tau_{tl32}\langle q\rangle^{+}_{3t},$$

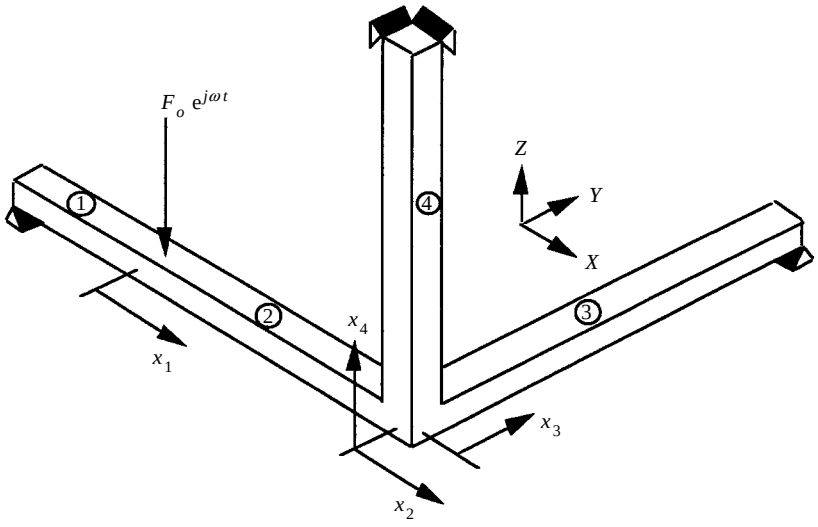

Figure 3. A frame structure with a three-dimensional joint.

$$\langle q\rangle^{-}_{2t} = r_{fzt22}\langle q\rangle^{+}_{2fz} + r_{fyt22}\langle q\rangle^{+}_{2fy} + r_{lt22}\langle q\rangle^{+}_{2l} + r_{tt22}\langle q\rangle^{+}_{2t} + \tau_{fxt42}\langle q\rangle^{+}_{4fx} + \tau_{fyt42}\langle q\rangle^{+}_{4fy}$$
$$+\tau_{lt42}\langle q\rangle^{+}_{4l} + \tau_{tt42}\langle q\rangle^{+}_{4t} + \tau_{fzt32}\langle q\rangle^{+}_{3fz} + \tau_{fxt32}\langle q\rangle^{+}_{3fx} + \tau_{lt32}\langle q\rangle^{+}_{3l} + \tau_{tt32}\langle q\rangle^{+}_{3t},$$
$$\langle q\rangle^{-}_{4fx} = \tau_{fzfx24}\langle q\rangle^{+}_{2fz} + \tau_{fyfx24}\langle q\rangle^{+}_{2fy} + \tau_{lfx24}\langle q\rangle^{+}_{2l} + \tau_{tfx24}\langle q\rangle^{+}_{2t} + r_{fxfx44}\langle q\rangle^{+}_{4fx}$$
$$+ r_{fyfx44}\langle q\rangle^{+}_{4fy} + r_{lfx44}\langle q\rangle^{+}_{4l} + r_{tfx44}\langle q\rangle^{+}_{4t} + \tau_{fzfx34}\langle q\rangle^{+}_{3fz}$$
$$+ \tau_{fxfx34}\langle q\rangle^{+}_{3fx} + \tau_{lfx34}\langle q\rangle^{+}_{3l} + \tau_{tfx34}\langle q\rangle^{+}_{3t},$$
$$\langle q\rangle^{-}_{4fy} = \tau_{fzfy24}\langle q\rangle^{+}_{2fz} + \tau_{fyfy24}\langle q\rangle^{+}_{2fy} + \tau_{lfy24}\langle q\rangle^{+}_{2l} + \tau_{tfy24}\langle q\rangle^{+}_{2t} + r_{fxfy44}\langle q\rangle^{+}_{4fx}$$
$$+ r_{fyfy44}\langle q\rangle^{+}_{4fy} + r_{lfy44}\langle q\rangle^{+}_{4l} + r_{tfy44}\langle q\rangle^{+}_{4t} + \tau_{fzfy34}\langle q\rangle^{+}_{3fz}$$
$$+ \tau_{fxfy34}\langle q\rangle^{+}_{3fx} + \tau_{lfy34}\langle q\rangle^{+}_{3l} + \tau_{tfy34}\langle q\rangle^{+}_{3t},$$
$$\langle q\rangle^{-}_{4l} = \tau_{fzl24}\langle q\rangle^{+}_{2fz} + \tau_{fyl24}\langle q\rangle^{+}_{2fy} + \tau_{ll24}\langle q\rangle^{+}_{2l} + \tau_{tl24}\langle q\rangle^{+}_{2t} + r_{fxl44}\langle q\rangle^{+}_{4fx} + r_{fyl44}\langle q\rangle^{+}_{4fy}$$
$$+r_{ll44}\langle q\rangle^{+}_{4l} + r_{tl44}\langle q\rangle^{+}_{4t} + \tau_{fzl34}\langle q\rangle^{+}_{3fz} + \tau_{fxl34}\langle q\rangle^{+}_{3fx} + \tau_{ll34}\langle q\rangle^{+}_{3l} + \tau_{tl34}\langle q\rangle^{+}_{3t},$$

and

$$\langle q\rangle^{-}_{4t} = \tau_{fzt24}\langle q\rangle^{+}_{2fz} + \tau_{fyt24}\langle q\rangle^{+}_{2fy} + \tau_{lt24}\langle q\rangle^{+}_{2l} + \tau_{tt24}\langle q\rangle^{+}_{2t} + r_{fxt44}\langle q\rangle^{+}_{4fx} + r_{fyt44}\langle q\rangle^{+}_{4fy}$$
$$+r_{lt44}\langle q\rangle^{+}_{4l} + r_{tt44}\langle q\rangle^{+}_{4t} + \tau_{fzt34}\langle q\rangle^{+}_{3fz} + \tau_{fxt34}\langle q\rangle^{+}_{3fx} + \tau_{lt34}\langle q\rangle^{+}_{3l} + \tau_{tt34}\langle q\rangle^{+}_{3t}, \quad (15)$$

where t_{mnij} is the wave type n power transmission coefficient in beam j due to the incident wave type m in beam i ($i, j = 2, 3, 4$; $m, n =$ two flexural ($f_y, f_z; f_x, f_z; f_x, f_y$), one longitudinal ($l$), and one torsional ($t$)) and r_{mnii} is the wave type n power reflection coefficient due to the incident wave type m in beam i. For example, the flexural component in the z-direction of the energy flow in beam section 3 in the positive direction, $\langle q\rangle^{-}_{3fz}$, is the sum of the contributions from 12 incident waves. Generally, a three-dimensional n-branch beam system uses $4n$ coupling relationships similar to equation (14) at the branched joint.

At the boundaries where there are no structural elements attached, there can be no vibrational energy flowing out of the boundaries. All the vibrational energy incident upon these boundaries will be reflected. Hence, the energy flow boundary condition,

$$\langle q\rangle^{+}_{ni} = \langle q\rangle^{-}_{ni}, \quad (16)$$

is applied for all wave components of energy flow at these boundaries. Hence, there are a total of 32 boundary conditions to be applied, which results in 32 simultaneous equations for coefficients A and B in equations (10) and (11), respectively, for four wave types in each of four beam sections.

3. "EXACT" ENERGETICS

The results predicted using EFA are verified using the frequency-averaged "exact" energetics of the frame structure. The "exact" energy density and energy flow expressions were obtained from the displacement solutions of one-dimensional wave equations of the various wave types.

The transverse displacement in beams can be represented as

$$w_{mi}(x_i) = A_{mi}\exp(-jk_{fmi}x_i) + B_{mi}\exp(-k_{fmi}x_i) + C_{mi}\exp(jk_{fmi}x_i) + D_{mi}\exp(k_{fmi}x_i), \quad (17)$$

where the subscript m is the direction of transverse displacement ($m = x$, y or z), the subscript i is the section of the beam structure ($i = 1$, 2, 3 or 4), and k_{fmi} is the complex flexural wavenumber. On the right-hand side of equation (17), the first term, $A_{mi}\exp(-jk_{fmi}x_i)$, represents the forward propagating flexural wave, the second term,

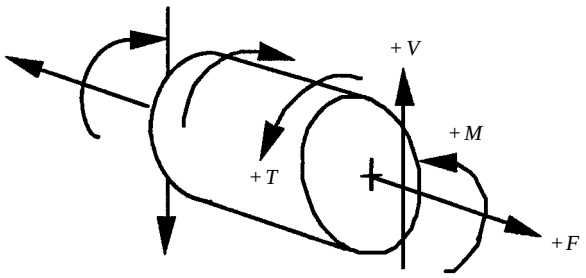

Figure 4. The sign conventions for positive torque, moments, shear, and axial forces.

$B_{mi}\exp(-k_{fmi}x_i)$, represents the forward decaying nearfield, the third term, $C_{mi}\exp(jk_{fmi}x_i)$, represents the backward propagating flexural wave, and the fourth term, $D_{mi}\exp(k_{fmi}x_i)$, represents the backward decaying nearfield.

The longitudinal displacement in beams can be represented as

$$u_i(x_i) = P_{li}\exp(-jk_{li}x_i) + Q_{li}\exp(jk_{li}x_i), \tag{18}$$

where k_{li} is the complex longitudinal wavenumber. On the right-hand side of equation (18), the first term, $P_{li}\exp(-jk_{li}x_i)$, represents the forward propagating longitudinal wave and the second term, $Q_{li}\exp(jk_{li}x_i)$, represents the backward propagating longitudinal wave.

The torsional displacement in beams can be represented as

$$\theta_i(x_i) = P_{ti}\exp(-jk_{ti}x_i) + Q_{ti}\exp(jk_{ti}x_i), \tag{19}$$

where k_{ti} is the complex torsional wavenumber. On the right-hand side of equation (19), the first term, $P_{ti}\exp(-jk_{ti}x_i)$, represents the forward propagating torsional wave and the second term, $Q_{ti}\exp(jk_{ti}x_i)$, represents the backward propagating torsional wave. The sign conventions used to derive the energy per unit length and energy flow expressions of various wave types are shown in Figure 4. The solution is found by solving a set of 48 simultaneous equations for coefficients in equations (17) through (19) for four wave types in each of four beam sections.

For harmonic excitation, the time-averaged energy per unit length and energy flow due to the flexural waves in beams are

$$\langle e\rangle_f = \tfrac{1}{4}EI\left\{\frac{\mathrm{d}^2w}{\mathrm{d}x^2}\frac{\mathrm{d}^2w^*}{\mathrm{d}x^2}\right\} + \tfrac{1}{4}\rho S\left\{\frac{\mathrm{d}w}{\mathrm{d}t}\frac{\mathrm{d}w^*}{\mathrm{d}t}\right\} \tag{20}$$

and

$$\langle q\rangle_f = \tfrac{1}{2}EI\ \mathrm{Re}\left\{\frac{\mathrm{d}^3w}{\mathrm{d}x^3}\frac{\mathrm{d}w^*}{\mathrm{d}t} - \frac{\mathrm{d}^2w}{\mathrm{d}x^2}\frac{\mathrm{d}^2w^*}{\mathrm{d}x\,\mathrm{d}t}\right\}. \tag{21}$$

The time-averaged energy per unit length and energy flow due to the longitudinal waves in beams are

$$\langle e\rangle_l = \tfrac{1}{4}ES\left\{\frac{\mathrm{d}u}{\mathrm{d}x}\frac{\mathrm{d}u^*}{\mathrm{d}x}\right\} + \tfrac{1}{4}\rho S\left\{\frac{\mathrm{d}u}{\mathrm{d}t}\frac{\mathrm{d}u^*}{\mathrm{d}t}\right\} \tag{22}$$

and

$$\langle q \rangle_t = \tfrac{1}{2} \operatorname{Re} \left\{ -ES \frac{\mathrm{d}u}{\mathrm{d}x} \frac{\mathrm{d}u^*}{\mathrm{d}t} \right\}. \tag{23}$$

The time-averaged energy per unit length and energy flow due to the torsional waves in beams are

$$\langle e \rangle_t = \tfrac{1}{4} T \left\{ \frac{\mathrm{d}\theta}{\mathrm{d}x} \frac{\mathrm{d}\theta^*}{\mathrm{d}x} \right\} + \tfrac{1}{4} J \left\{ \frac{\mathrm{d}\theta}{\mathrm{d}t} \frac{\mathrm{d}\theta^*}{\mathrm{d}t} \right\} \tag{24}$$

and

$$\langle q \rangle_t = \tfrac{1}{2} \operatorname{Re} \left\{ -T \frac{\mathrm{d}\theta}{\mathrm{d}x} \frac{\mathrm{d}\theta^*}{\mathrm{d}t} \right\}, \tag{25}$$

where T is the torsional stiffness and J is the mass moment of inertia. The frequency averaged "exact" energetics are obtained using the relationships

$$\langle \hat{e} \rangle = \frac{1}{(\omega_2 - \omega_1)} \int_{\omega_1}^{\omega_2} \langle e \rangle \, \mathrm{d}\omega, \qquad \langle \hat{q} \rangle = \frac{1}{(\omega_2 - \omega_1)} \int_{\omega_1}^{\omega_2} \langle q \rangle \, \mathrm{d}\omega. \tag{26, 27}$$

In this investigation, the difference in frequency, $\omega_2 - \omega_1$, will be a one-third octave band.

4. RESULTS

EFA is used here to predict the energetics of the frame structure shown in Figure 3. The equivalent energy flow problem is shown in Figure 5. The EFA results are compared to

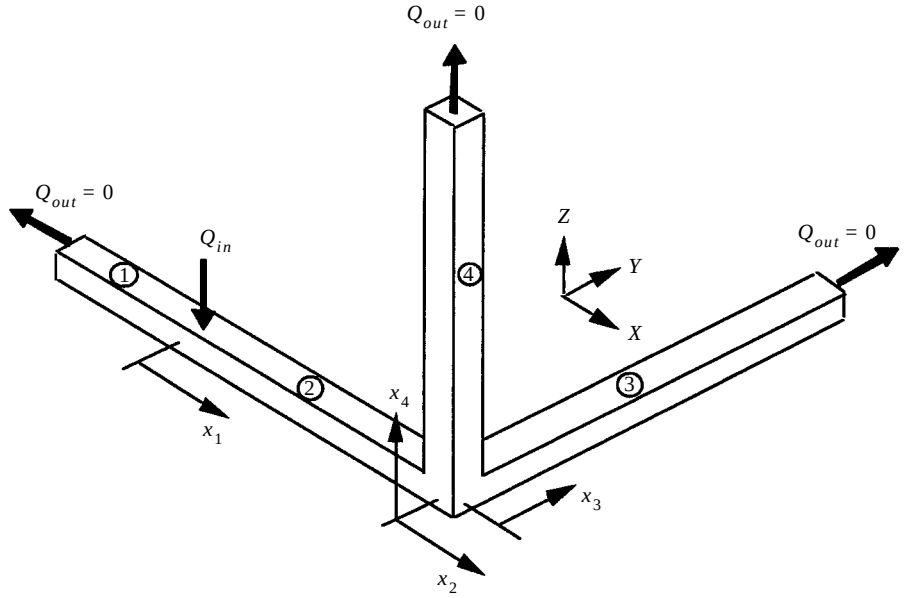

Figure 5. Equivalent energy problem.

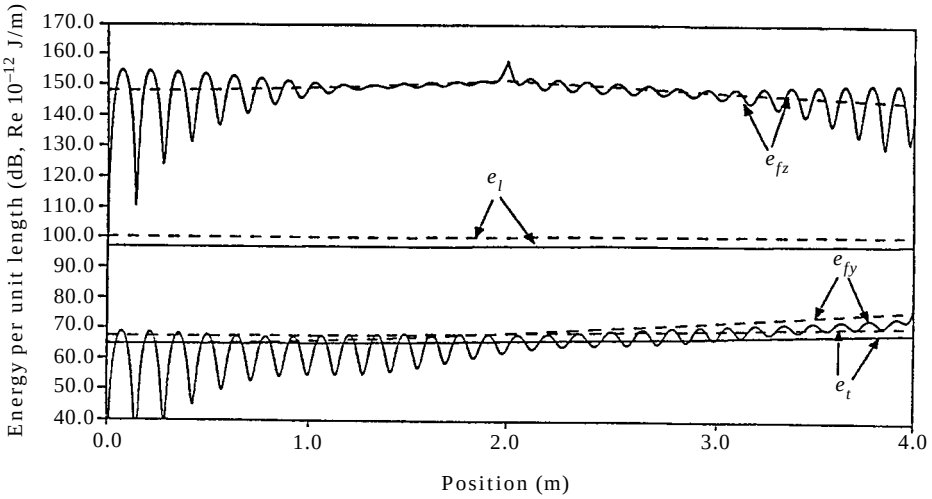

Figure 6. Comparison of the four components of the "exact" energy density frequency-averaged over the 2500 Hz one-third octave band and the energy density predicted by EFA at $f_c = 2500$ Hz in beam sections 1 and 2; ——, "exact" response; ----, EFA prediction.

the frequency-averaged "exact" energetics. All beams are made of aluminum ($E = 7{\cdot}1 \times 1010$ Pa and $\rho = 2700$ kg/m^3). The cross-sectional area and the area moment of inertia are 4×10^{-4} m^2 and $1{\cdot}3333 \times 10^{-8}$ m^4, respectively, for all beams. The length of all beams is 4 m. The structural loss factor for all beams is 0·04. The magnitude of the applied point force in the incident beam is 10 N.

In Figures 6 and 7, the four components of the energy per unit length and energy flow (magnitude) predicted by EFA at the center frequency of 2500 Hz in beam sections 1 and 2 are compared to the four components of the "exact" energy per unit length and energy flow (magnitude) frequency averaged over the 2500 Hz one-third octave band. At the center frequency of 2500 Hz, the one-third octave bandwidth is 580 Hz. In Figure 7, all

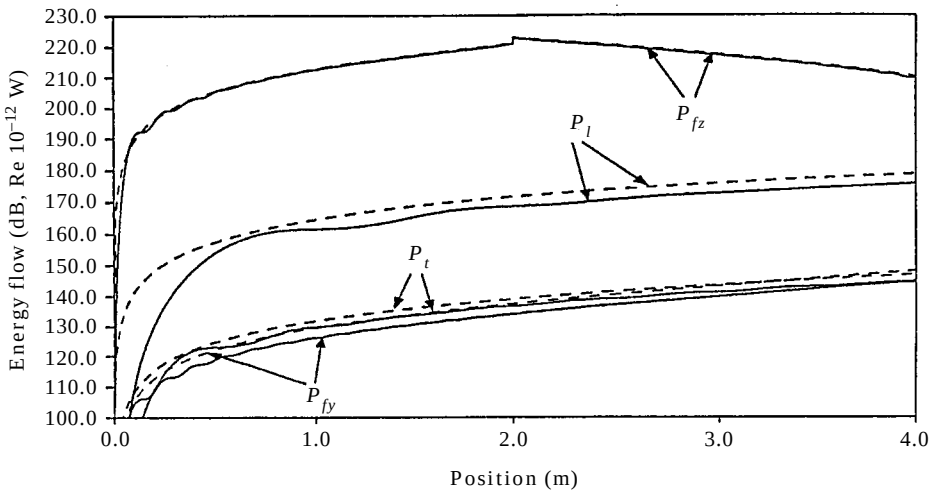

Figure 7. Comparison of the four components of the "exact" energy flow frequency-averaged over the 2500 Hz one-third octave band and the energy flow predicted by EFA at $f_c = 2500$ Hz in beam sections 1 and 2; ——, "exact" response; ----, EFA prediction.

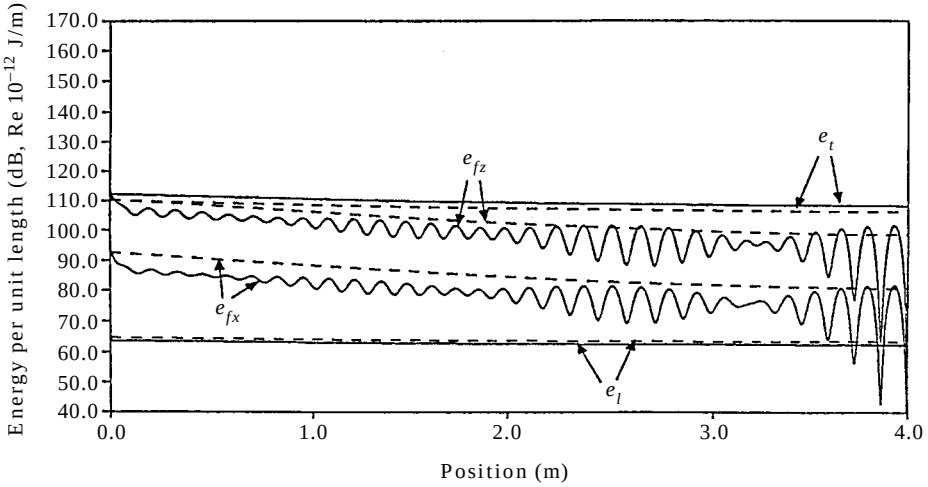

Figure 8. Comparison of the four components of the "exact" energy density frequency-averaged over the 2500 Hz one-third octave band and the energy density predicted by EFA at $f_c = 2500$ Hz in beam section 3; ——, "exact" response; ----, EFA prediction.

four components of the energy are flowing in the negative direction except for the z direction flexural energy flow, which is flowing in the positive direction from $x = 2$–4 m. In Figure 6, the sharp peak in the z direction flexural energy per unit length (e_{fz}) and, in Figure 7, the discontinuity of the z direction flexural energy flow (p_{fz}) at $x = 2$ m are at the location of the excitation source. The dominant energetics in the incident beam are the z direction flexural energetics. The secondary energetics are longitudinal energetics which are approximately 50 dB below the z direction flexural energetics. The torsional energetics and the y direction flexural energetics are not coupled well to the excitation source.

In Figures 8 and 9, the four components of the energy per unit length and energy flow (magnitude) predicted by EFA at the center frequency of 2500 Hz in beam section 3 are

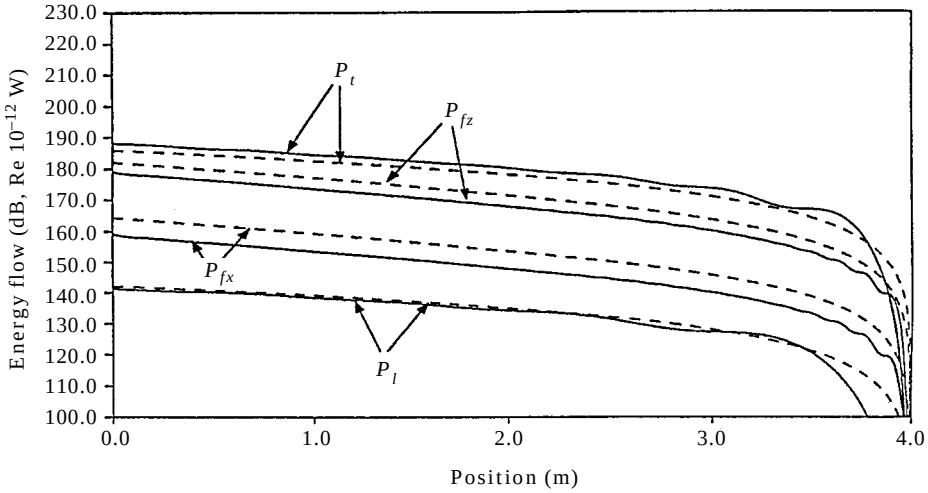

Figure 9. Comparison of the four components of the "exact" energy flow frequency-averaged over the 2500 Hz one-third octave band and the energy flow predicted by EFA at $f_c = 2500$ Hz in beam section 3; ——, "exact" response; ----, EFA prediction.

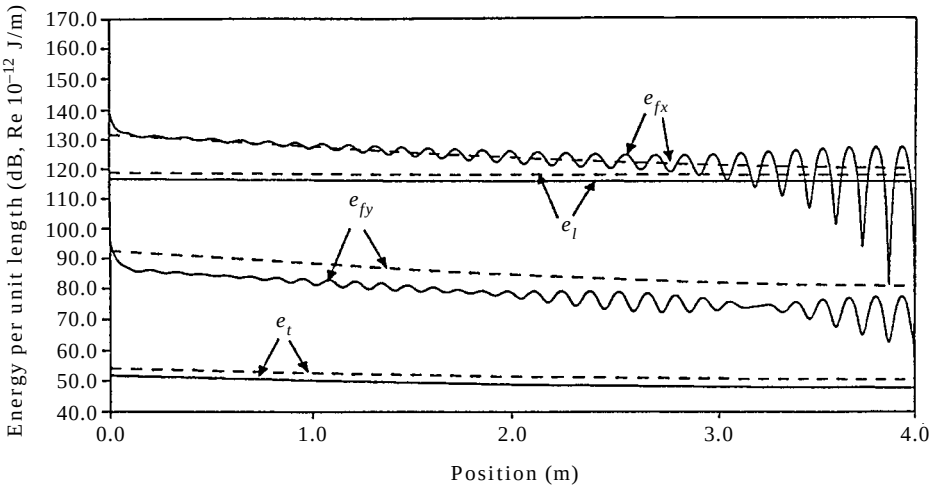

Figure 10. Comparison of the four components of the "exact" energy density frequency-averaged over the 2500 Hz one-third octave band and the energy density predicted by EFA at $f_c = 2500$ Hz in beam section 4; ——, "exact" response; ----, EFA prediction.

compared to the four components of the "exact" energy per unit length and energy flow (magnitude) frequency averaged over the 2500 Hz one-third octave band. The dominant energetics in beam section 3 are the torsional energetics. The secondary energetics are the z direction flexural energetics which are approximately 10 dB below the torsional energetics. In beam section 3, the x direction flexural energetics and the longitudinal energetics do not couple well with the dominant energetics of the other beam sections.

In Figures 10 and 11, the four components of the energy per unit length and energy flow (magnitude) predicted by EFA at the center frequency of 2500 Hz in beam section 4 are compared to the four components of the "exact" energy per unit length and energy flow (magnitude) frequency averaged over the 2500 Hz one-third octave band. The dominant energetics in beam section 4 are the x direction flexural energetics. The secondary

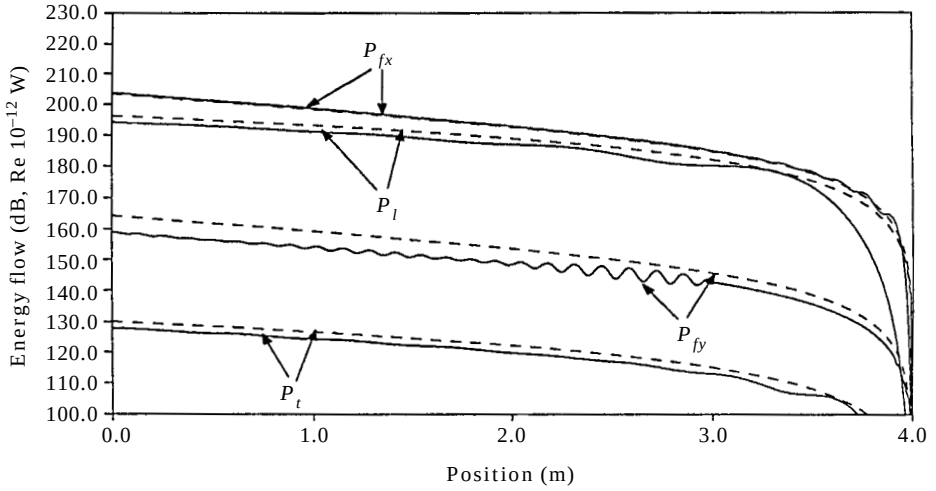

Figure 11. Comparison of the four components of the "exact" energy flow frequency-averaged over the 2500 Hz one-third octave band and the energy flow predicted by EFA at $f_c = 2500$ Hz in beam section 4; ——, "exact" response; ----, EFA prediction.

energetics are the longitudinal energetics, which are 10 dB below the x direction flexural energetics. In beam section 4, the y direction flexural energetics and the torsional energetics do not couple well with the dominant energetics of the other beam sections.

In Figures 6–11, the difference between the lowest and the highest of the four components of the energetics of any beam section is typically 70 dB. Even with this large variation, the essential behavior of the frame structure is well predicted by EFA. The dominant energetics in each beam section are predicted within 0·5–2 dB. The secondary energetics in each beam section, which are 10–50 dB below the dominant energetics, are predicted within 3–5 dB. The dominant energetics of the frame structure is the z direction flexural energetics in the incident beam. Other dominant energetics in other beam sections are typically 30 dB below the z direction flexural energetics in the incident beam. EFA shows that the three-dimensional joint is not an efficient transmitter of energy to other beam sections in the frame structure in this frequency band.

Cho [17] shows an additional case study of the same frame structure for the 4000 Hz one-third octave band where exact results are compared to EFA predictions. The results improve compared to the results shown here for the 2500 Hz one-third octave band because the reflection and transmission coefficients of semi-infinite systems are better approximations of the reflection and transmission of finite systems at higher frequencies.

5. CONCLUSIONS

An EFA method is developed for predicting the frequency-averaged energy per unit length and energy flow distributions in built-up structures. EFA is used to predict the vibrational response of a frame structure with a three-dimensional joint. The predictions made by EFA are a good frequency-averaged approximation of the "exact" energetics. Also, the dominant energy transmission mechanisms in the frame structure were identified using EFA. Work is currently underway for applying EFA to a real built-up structure with complicated geometry and shape using an energy based finite element method (EFEM).

ACKNOWLEDGMENTS

The authors would like to thank the Lord Corporation, NASA Langley Research Center, and Ford Motor Company for financial support of this investigation.

REFERENCES

1. M. S. Kompella and R. J. Bernhard 1993 *Proceedings of SAE Noise & Vibration Conference*, *SAE Paper* 931272, *Traverse City*, *U.S.A.*, 65–77. Variation of structural–acoustic characteristics of automotive vehicles.
2. L. A. Wood and C. A. Joachim 1987 *International Journal of Vehicle Design* **8**, 428–438. Interior noise scatter in four-cylinder sedans and wagons.
3. D. J. Nefske and S. H. Sung 1989 *Journal of Vibration*, *Acoustics*, *Stress*, *and Reliability in Design* **111**, 94–100. Power flow finite element analysis of dynamic systems: basic theory and application to beams.
4. J. C. Wohlever and R. J. Bernhard 1992 *Journal of Sound and Vibration* **153**, 1–19. Mechanical energy flow models of rods and beams.
5. O. M. Bouthier and R. J. Bernhard 1995 *Journal of Sound and Vibration* **182**, 129–147. Simple models of energy flow in membranes.
6. O. M. Bouthier and R. J. Bernhard 1995 *Journal of Sound and Vibration* **182**, 149–164. Simple models of the energetics of transversely vibrating plates.
7. P. E. Cho and R. J. Bernhard 1992 *Proceedings of Inter-Noise* 92, *Toronto*, *Canada*, 487–492. Coupling of continuous models of beams.

8. P. E. Cho and R. J. Bernhard 1993 *Proceedings of* 4*th International Congress on Intensity Techniques*, *Senlis*, *France*, 347–354. A simple method for predicting energy flow distributions in frame structures.
9. R. H. Lyon 1975 *Statistical Energy Analysis of Dynamic Systems*: *Theory and Applications*. Cambridge, MA: MIT Press.
10. F. J. Fahy 1974 *The Shock and Vibration Digest*, 14–33. Statistical energy analysis: a critical review.
11. J. Woodhouse 1981 *Applied Acoustics* **14**, 455–469. An introduction to statistical energy analysis of structural vibration.
12. M. J. Sablik 1982 *Journal of the Acoustical Society of America* **72**, 1285–1288. Coupling loss factors at a beam L-joint revisited.
13. L. Cremer, M. Heckl and E. E. Ungar 1988 *Structure-Borne Sound*. Berlin: Springer.
14. J. L. Horner and R. G. White 1991 *Journal of Sound and Vibration* **147**, 87–103. Prediction of vibrational power transmission through bends and joints in beam-like structures.
15. J. F. Doyle and S. Kamle 1987 *Journal of Applied Mechanics* **54**, 136–140. An experimental study of the reflection and transmission of flexural waves at an arbitrary T-joint.
16. D. U. Noiseux 1970 *Journal of the Acoustical Society of America* **47**, 238–247. Measurement of power flow in uniform beams and plates.
17. P. E. Cho 1993 *PhD Thesis*, *Purdue University*. Energy flow analysis of coupled structures.